

Runoff and water budget of the Liudaogou Catchment at the wind–water erosion crisscross region on the Loess Plateau of China

Huang Jinbai · Wen Jiawei ·
Hinokidani Osamu · Yasuda Hiroshi

Received: 28 July 2013 / Accepted: 7 April 2014 / Published online: 24 April 2014
© Springer-Verlag Berlin Heidelberg 2014

Abstract The objectives of this study were to examine the runoff characteristics and to estimate water budget at the wind–water erosion crisscross region on the Loess Plateau of China. A small catchment known as Liudaogou that has representative meteorological and hydrological conditions of the wind–water erosion crisscross region was chosen as the study location. A numerical model for rainfall–runoff was developed and verified; rainfall–runoff calculation for 5 years (2005–2009) was performed. The observed data and numerical result of the surface runoff were used for evaluating runoff characteristics and estimating the annual water budget. Runoff rate was proportional to average intensity of rain. Even though rainfall duration was for few minutes, surface runoff was generated

by intensity of more than $2.6 \text{ mm} \times 5 \text{ min}^{-1}$, when rainfall duration exceeded 10 h; surface runoff was generated by an intensity of $0.6 \text{ mm} \times 5 \text{ min}^{-1}$, while annual runoff rate was 10–15 %. The unit area of 1 km^2 was adopted as the index area for estimating annual water budget. Runoff, evapotranspiration, variation of water storage, and habitant water consumption accounted for 20.4, 75.6, 0, and 4 % of the total annual precipitation, respectively. Results of this study provide the basis for further research on hydrology, water resources, and sustainable water development and utilization at the wind–water erosion crisscross region on the northern Loess Plateau where annual water resources are relatively deficient.

Keywords Loess Plateau · Wind–water erosion crisscross region · Liudaogou Catchment · Runoff · Water budget

Electronic supplementary material The online version of this article (doi:10.1007/s12665-014-3273-y) contains supplementary material, which is available to authorized users.

H. Jinbai (✉)
College of Hydraulic Science and Engineering,
Yangzhou University, No. 31, Jiangyang-Middle Road,
Yangzhou 225009, China
e-mail: huangjinbai@aliyun.com

W. Jiawei
College of Information Engineering, Yangzhou University,
No. 88, South University Road, Yangzhou 225009, China
e-mail: wenjiawei@aliyun.com

H. Osamu
Faculty of Engineering, The Graduate School, Tottori
University, 4-101, Koyama-Minami, Tottori 680-8552, Japan
e-mail: hinokida@cv.tottori-u.ac.jp

Y. Hiroshi
Arid Land Research Center, Tottori University, 1390, Hamasaka,
Tottori 680-0001, Japan
e-mail: hyasd@alrc.tottori-u.ac.jp

Introduction

Chinese Loess Plateau is well-known for its serious soil erosion largely caused by cultivation of marginal lands and destruction of natural vegetation (Shi and Shao 2000; Lu and van Ittersum 2004). As a vast semiarid and high-risk region of desertification, this region has been a great concern not only in China but also in the world. In the process of desertification, serious soil erosion has occurred on the Loess Plateau since the 17th century (Wang and Takahashi 1999; Bo and Long 2002). Soil and water loss has seriously depleted land resources and degraded the eco-environment in the Loess plateau (Shi and Shao 2000). Revegetation is recognized as an important means to control soil erosion and protect land from desertification (Bu et al. 2002; Jia et al. 2010). Although water is a key factor for restoration of vegetation (Li 1983; Huo et al. 2008), however, scarce and

uneven distribution of rainfall in addition to intense evapotranspiration causes the deficiency of annual water resources (Zheng et al. 2005; Kimura et al. 2005a) which hampering restoration of vegetation in the Loess Plateau (Yang 1996).

The northern Loess Plateau is a fragile ecological environment in China due to severe soil erosion and serious ecosystem degradation (Yang and Shao 1998; Tang 2000), and tendency of desertification at the northern region has become more severe than that at the southern region in the Loess Plateau due to the long-term water and wind crisscross erosion compounded by low precipitation. Ecological restoration and sustainable agriculture are hardly guaranteed by the limited water resources at the wind–water erosion crisscross region of the northern Loess Plateau.

Guaranteeing agricultural production and ecological restoration in the Loess Plateau relies on available water resources (Chen et al. 2007). Researches on water budget are significant for estimating seasonal water resources and hydrological circle within a basin. Meanwhile, runoff is a basic hydrological factor when estimating water budget, thereby, clarification of runoff characteristics is also important for further studies on hydrological circle and estimating water resources. The conventional studies related to water resources have been conducted at the wind–water erosion crisscross region on the northern Loess Plateau. Kimura et al. (2004, 2007) estimated the moisture availability over the Liudaogou Catchment using new indices with surface temperature; Zhu and Shao (2008) characterized variability and the pattern of upper soil moisture by field experiment; Fan et al. (2010) evaluated the soil water balance during vegetative restoration; Hu et al. (2011) characterized the spatio-temporal variability behavior of land surface soil water. Research focusing on evapotranspiration also has been conducted at this catchment such as by Kimura et al. (2005b, 2007), Wang et al. (2010). Compared to research findings related to soil water and evapotranspiration, the runoff characteristics and water budget are still poorly understood due to lack of the studies even though such studies are significant for assessing the available water resources of the study location. This study was therefore conducted at the Liudaogou Catchment with the aims to reveal the main runoff characteristics and to estimate the water budget of the wind–water erosion crisscross region on the northern Loess Plateau.

Materials and methods

Study area

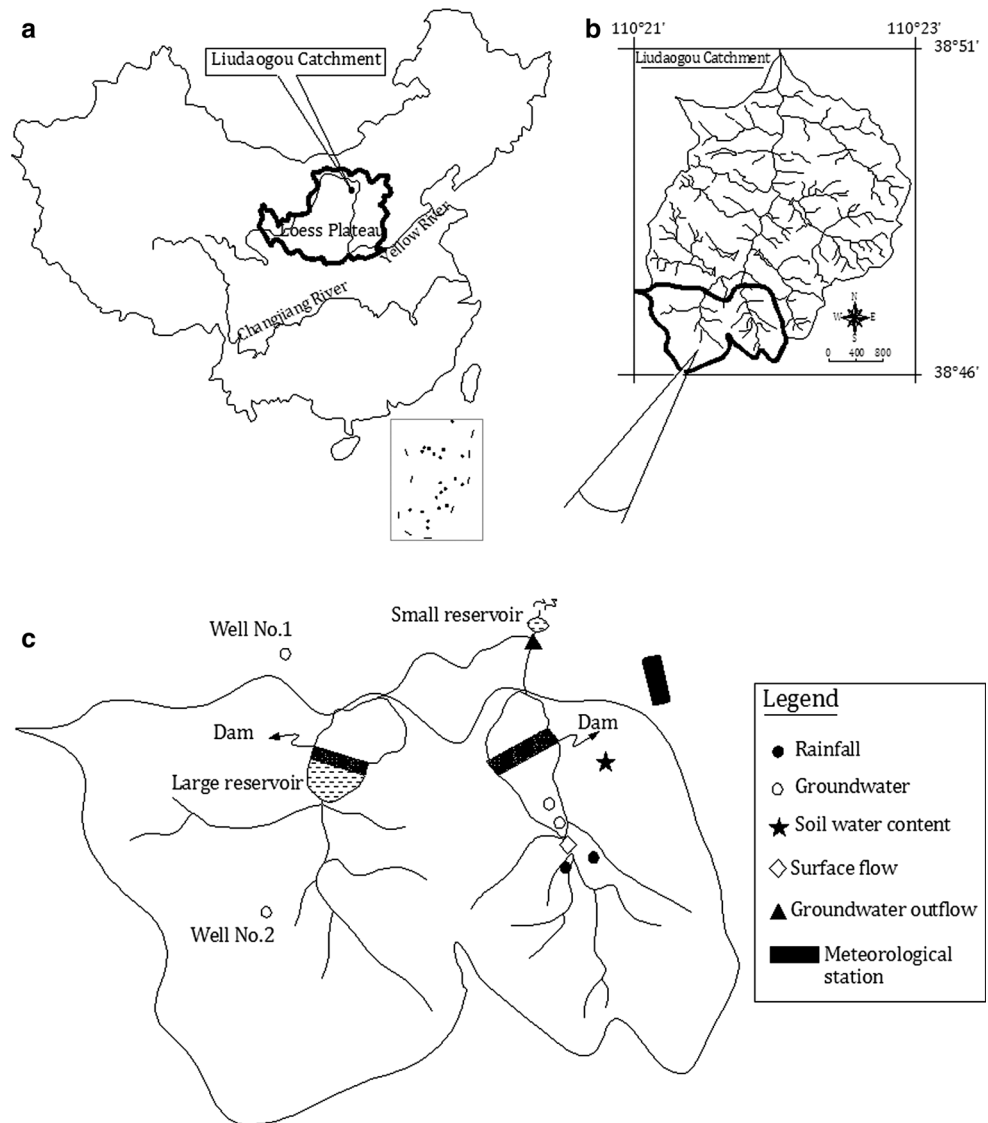
The Liudaogou Catchment (110°21′–110°23′E longitude and 38°46′–38°51′N latitude, area: 6.89 km²) (Fig. 1) was chosen as the study location because it represents diversified

landscape types in terms of geology, morphology, soil, hydrology and climatic conditions, and it represents a certain number of different land use patterns of the wind–water erosion crisscross region on the northern Loess Plateau environment (Huo et al. 2008; Zhu et al. 2008). This catchment is situated at the elevation ranging from 1,094.0 to 1,273.9 m above sea level. Average annual rainfall is 430 mm with uneven seasonal distribution, more than 70 % of the total rainfall is received in the rainy season from June to September. Annual potential evapotranspiration generally exceeds 1,000 mm. Terrain is considerably complicated, many gullies in various scales spread around the main river channel. Due to excessive pasturage, serious land erosion has occurred and the natural bush is severely damaged and there is almost no large area of distribution. Vegetation cover only accounts for about 25 % of the total basin area (Jiang et al. 2005; Fan et al. 2006).

Data acquisition

The data used for analysis were obtained mainly through field observations. Hydrological and meteorological observations were conducted on the Liudaogou Catchment. Hydrological observations included rainfall, groundwater level, soil water content, discharge of surface flow in river channel, and groundwater outflow. The tipping rain gauge [Model number: 7852 M-L10, Dimensions: $\phi 165 \times 240$ (mm)] was used for rainfall observation and rain gauge of this type records data once for every 0.2 mm rainfall. Groundwater level (phreatic water) and the depth of the surface flow were observed by water level recorder (Groundwater level, HM-910-02-309, *Sensez co. ltd.*; Surface flow, KADEC21-MZPT, *KONA System co. ltd.*). Discharge of groundwater outflow was observed by a flow meter (Model number: KENEK-VE20). Observation on soil water content was conducted by soil moisture sensor (Model number: S-SMC-M005, *HOB0 Data Loggers*). As the groundwater level was relatively stable, the measurement interval was set to 1 h. The measurement interval of the surface flow observation was set to 5 min considering the ephemeral runoff was significantly influenced by rainfall intensity. To estimate the surface flow, the water level data were converted into discharge data. Manning's mean velocity formula was applied to the conventional method for data transformation from water level to discharge (Eq. 2). Meteorological observations such as temperature, sunshine duration, wind speed, atmospheric pressure, and air humidity were also carried out at a meteorological station which was set up at the upstream of the Liudaogou Catchment. Layout of the field observation management was represented in Fig. 1c. Field observation was conducted since May in 2004, however, data deficiency in various degrees existed during the observed period due to influence by uncertain factors.

Fig. 1 Position of the study location and layout of field observation management. **a** Location of Loess Plateau in China and the Liudaogou Catchment in Loess Plateau. **b** Position of the Liudaogou Catchment. **c** Layout of field observation management



Numerical model for runoff calculation

The results on hydro-geological survey indicate that topsoil is loose loess with thickness of about 10–15 cm on the slope, subsequent to the topsoil, the soil profile is hard yellow ocher with thickness down to 20 m depth, the groundwater table (phreatic water) exists below the second soil layer. The under stratum is sandstone formed in the Jurassic period of Mesozoic. Model of the vertical profile of soil on the slope was therefore considered to be composed of two layers (Fig. 2). As there is no loose topsoil in the river channel, the set up of the soil layer from the ground surface to the groundwater table in the model was the single layer. Model lumping of the general hydro-geological conditions of the Liudaogou Catchment is depicted in Fig. 2.

Ephemeral runoff is restrictively generated only for intensive rainfall in the rainy season at the wind–water erosion crisscross region of the Loess Plateau. In this study,

surface runoff was estimated using rainfall-runoff numerical model. Various models on rainfall-runoff calculation have been conventionally proposed such as the prior representative models: System Hydrologic European (SHE, Abbott et al. 1986), Institute of Hydrology Distributed model (IHDM, Calver and Wood 1995), Topographic Kinematic Approximation and Integration (TOPKAPI, Ciarapica and Todini 2002), Soil and Water Assessment Tools (SWAT, Neitsch et al. 2000) and etc. Delfs et al. (2013) proposed a practical model in which coupled surface/subsurface flow model accounting for air entrapment and air pressure counterflow. To achieve accurate numerical calculation on runoff at the study location and to provide a practical numerical model for rainfall-runoff process for the Liudaogou Catchment, a numerical model was originally developed based on kinematic wave theory combined river channel network for rainfall-runoff process calculation for the distributive basin (Huang et al. 2008).

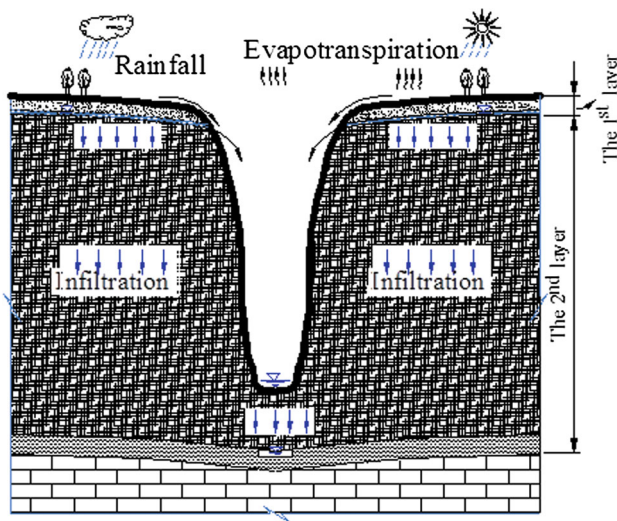


Fig. 2 Model lumping of hydro-geological conditions of the Liudaogou Catchment

The kinematic wave equations are used widely in calculating the rainfall-runoff process as it is physically based and utilizes physical parameters to characterize a basin. Kinematic model is also applied to describe the features of infiltration and subsurface lateral flows (Mariza et al. 1992; Yomoto and Mohammad 1992; Chua Lloyd et al. 2008). Sarkar and Dutta (2012) used the kinematic form of Darcy's equation to formulate subsurface flow. To apply the kinematic model, lumping of the basin is necessary because of the physical characteristics, such as surface condition, roughness, and slope. So, characterization of the study area is required before the lumping (Huang et al. 2013).

Governing equations

The governing equations include equations of continuity, motion of one-dimensional surface flow (Eqs. 1 and 2), and infiltration flow (Eqs. 3 and 4) (used for the first layer in slope sector, Fig. 2).

$$\frac{\partial h}{\partial t} + \frac{\partial q}{\partial x} = r - f_1 \quad (1)$$

$$v = \frac{1}{n} R(h)^{\frac{2}{3}} I^{\frac{1}{2}} \quad (2)$$

$$\lambda \frac{\partial \bar{h}}{\partial t} + \frac{\partial \bar{q}}{\partial x} = f_1 - f_2 - ET \quad (3)$$

$$\bar{v} = k\bar{I} \quad (4)$$

where, h is depth of water (m), q is unit width flow discharge ($\text{m}^2 \text{s}^{-1}$), x is distance in flow direction (m), Δt is unit time (s), v is velocity of flow (m s^{-1}), r is effective rainfall (m s^{-1}), f_1 is mean infiltration velocity of the first soil layer (m s^{-1}), b is width of the river channel (m), n is

coefficient of the roughness ($\text{s m}^{-1/3}$), R is hydraulic radius (m), I is gradient of riverbed, λ is soil effective porosity, \bar{h} is depth of infiltration flow (m), \bar{q} is the discharge of infiltration flow of the unit width ($\text{m}^2 \text{s}^{-1}$), \bar{I} is gradient of the groundwater table of the first layer, f_2 is the mean infiltration velocity of the subsequent soil layer (m s^{-1}), ET is the evapotranspiration (m s^{-1}), \bar{v} is velocity of infiltration flow (m s^{-1}), k is coefficient of permeability (m s^{-1}).

The equations for calculation in the second soil layer were analogous with those of the first soil layer. Only the footnote number and the sectional form are replaced. The equations for the river channel are similar to those for the slope. Only some factors in the equations were replaced, which resulted in variation of the equations in forms.

Difference scheme

As the governing equations characterize the transfer of the boundary condition from upstream to downstream, the upstream difference scheme was used (Japan Society of Mechanical Engineers 1988). According to the upstream difference scheme, the continuity equation of the surface flow (Eq. 1) and the continuity equation of the groundwater flow (Eq. 3) were discretized as follows:

$$h_i^{n+1} = h_i^n + dt(r - f_1 - \frac{q_i^n - q_{i-1}^n}{dx}) \quad (5)$$

$$\bar{h}_i^{n+1} = \bar{h}_i^n + \frac{dt}{\lambda}(f_1 - f_2 - \frac{\bar{q}_i^n - \bar{q}_{i-1}^n}{dx}) \quad (6)$$

where, n is time step, i is spatial step in flow direction, and other factors correspond to those previously mentioned.

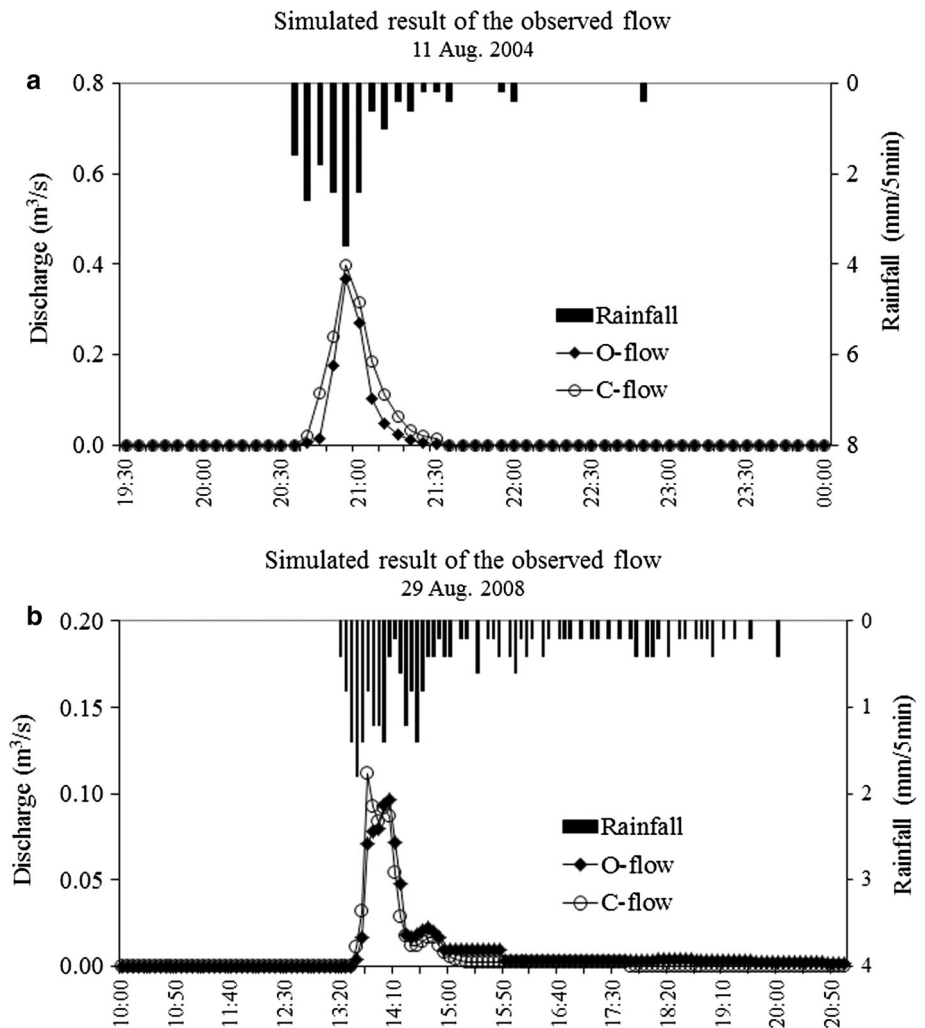
Initial and boundary conditions

As the initial condition, the discharges of the surface and groundwater flows were assumed as 0 at the upstream end (the origin of the flow) of each slope sector. In the process of the calculation, boundary condition was set to the calculation on infiltration velocity in the first and second soil layers which is given by water depth of the surface flow and infiltration flow in the first layer, respectively. For example, the infiltration velocity of the first layer (f_1) in Eq. (1) was equal to the depth of water (h_i) divided by the unit of time (dt) (h_i/dt) when $h_i/dt < f_1$.

Model validation

Validity of the numerical model for rainfall-runoff calculation at the Liudaogou Catchment was tested and verified in previous studies (Huang et al. 2008, 2011). The numerical results showed excellent fit with the observed data (Fig. 3). The discharge was observed at the surface

Fig. 3 The simulated results of the surface flow (*O-flow* observed flow discharge, *C-flow* calculated result). **a** 11 Aug. 2004. **b** 29 Aug. 2008



flow observation point (Fig. 1c). The difference between the calculated flow (C-flow in Fig. 3) and the observed flow (O-flow in Fig. 3) was <3 %. The model was therefore applied to rainfall-runoff calculation at the Liudaogou Catchment.

Numerical calculation for rainfall-runoff was carried out for 5 years (2005–2009); the numerical results of runoff were used for estimating annual runoff rate and evaluating water budget of the Liudaogou Catchment.

Results and discussion for runoff

Mechanism of runoff generation

Mechanism of runoff generation for saturated topsoil

Soil water content was also measured on the cross-section on which the surface flow was observed (Fig. 4). Figure 5 depicts the temporal process of rainfall, variation of soil water content at different depths and runoff on 15–16

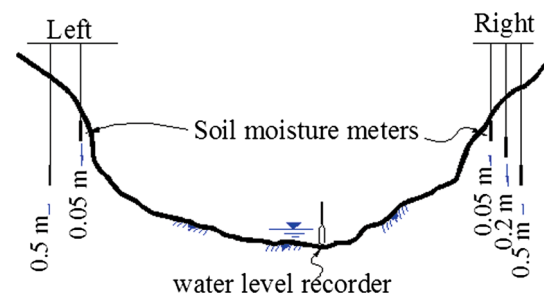


Fig. 4 Schematic drawing of the surface flow and soil water content observed section

August 2008. Rainfall amount is 86.2 mm, rainfall duration is 1,335 min, and the maximum rain intensity was 2.0 mm × 5 min⁻¹. During the lag from rainfall start and runoff generation, as the rain intensity was lower than unsaturated infiltration velocity of the topsoil, rainfall was entirely infiltrated into soil by assuming evapotranspiration was 0. Soil water content at the depth of 5 cm in both sides began to increase at the different time point, respectively. Soil water content at the depth of 20 cm increased later

than that of the depth of 5 cm, however, soil water content at 50 cm always remained stable before runoff generation. Runoff was generated by rain intensity of $0.6 \text{ mm} \times 5 \text{ min}^{-1}$. At the time of runoff came into being, soil water content at the depth of 20 cm increased distinctly, whereas at the depth of 50 cm, its change was not clear. As rain intensity of $1.2 \text{ mm} \times 5 \text{ min}^{-1}$ once occurred before runoff generation and the lag between start of rain and runoff generation was more than 10 h, topsoil attained saturation when runoff was generated (Fig. 5). Additionally, before the runoff generation, the accumulated amount of infiltration was 27.0 mm which was given by the initial loss assuming no evaporation. As the porosity of the

topsoil was 0.30–0.35 at the surface flow, observed location thickness of the topsoil was estimated to be about 8 cm.

Another representative long duration with low intensity rainy event occurred on 14–15 August 2004 (Fig. 1, ESM only). In this rainy event, the rain duration was 735 min, total rainfall was 44.2 mm, and the maximum intensity was $0.8 \text{ mm} \times 5 \text{ min}^{-1}$ before runoff generation. Runoff was generated by rain intensity of $0.6 \text{ mm} \times 5 \text{ min}^{-1}$. Before runoff generation, rainfall of 22.6 mm was infiltrated into the soil. Topsoil was inferred to attain saturated conditions because the lag from rainfall start to runoff generation was more than 10 h. Therefore, mechanism of saturation excess

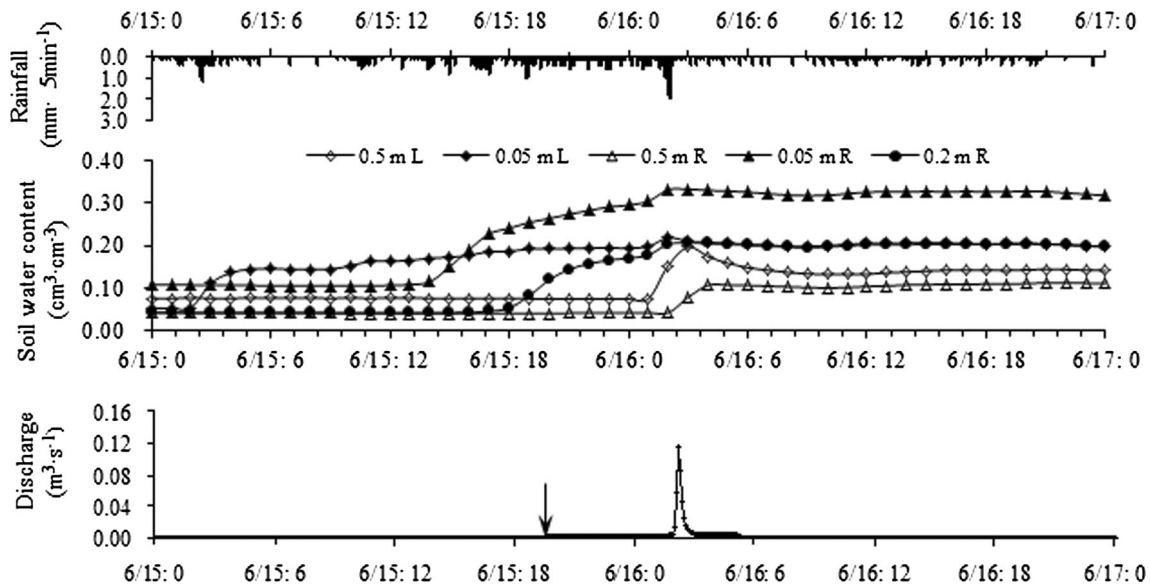


Fig. 5 Mechanism of runoff generation due to a long duration and low intensity rainfall (15–16 Aug. 2008) (arrow points out to the time when the runoff occurred)

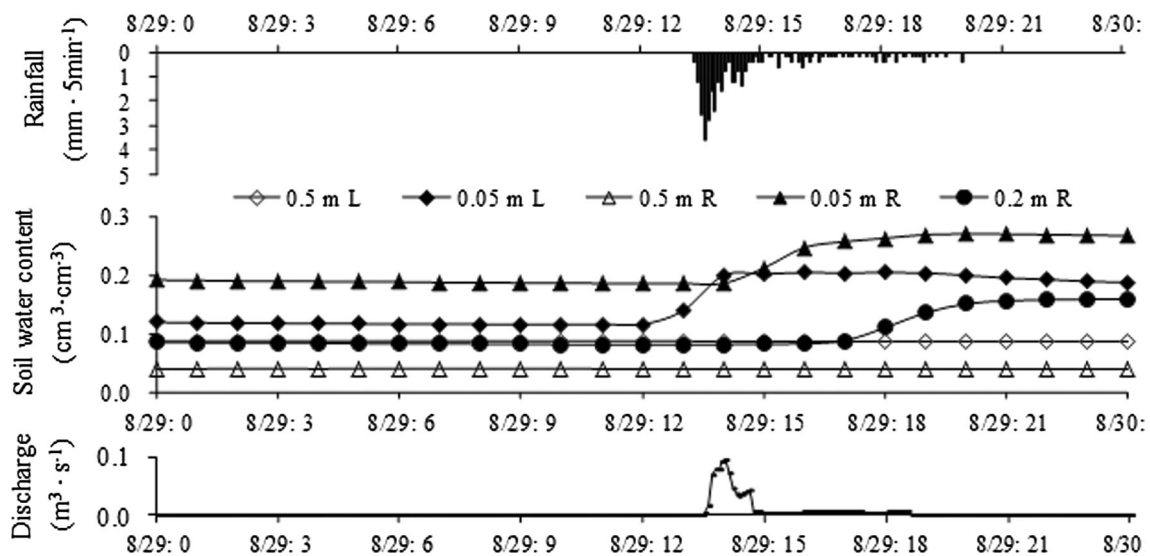


Fig. 6 Mechanism of runoff generation caused by a short duration and high intensity rainfall (29 Aug. 2008)

Table 1 Index of rainfall of runoff events for unsaturated condition

Date	11 Aug. 2004	15 Aug. 2005	9 Jun. 2006
Rain duration (min)	80	60	30
Max. intensity (mm/5 min)	3.6	2.6	2.6
Total rainfall (mm)	18.4	14.0	6.0
Intensity when runoff started (mm/5 min)	2.6	2.6	2.6
Lag time from start of rainfall to runoff generation (min)	5	20	5

runoff can be concluded that the topsoil attained saturation and rain intensity is $\geq 0.6 \text{ mm} \times 5 \text{ min}^{-1}$.

Mechanism of runoff generation for unsaturated topsoil

Figure 6 depicts temporal process of rainfall, variation of soil water content and runoff which occurred on 29 August 2008. Rainfall was mainly concentrated between the time periods of 14:00–15:00 with an average intensity over $5.0 \text{ mm} \times 5 \text{ min}^{-1}$. Runoff was immediately generated by a rain intensity of $4.2 \text{ mm} \times 5 \text{ min}^{-1}$ at the time point of 10 min after rainfall started. Soil water content at various depths still remained relatively stable when runoff was being generated. Mechanism of runoff generation caused by high intensity rainfall can be simply generalized to postulate that runoff is consequentially generated by high rain intensity in spite of soil water content in the topsoil.

Three rainfall-runoff events that occurred on 11 August in 2004, 15 August in 2005, and 9 June in 2006 were chosen to evaluate the relationship between intensity of rain and runoff generation under unsaturated topsoil. The rainfall duration, rainfall amount, the maximum intensity, and the factors related to runoff generation are listed in Table 1. In all of the three rainfall events, runoff started immediately when intensity of rain attained $2.6 \text{ mm} \times 5 \text{ min}^{-1}$. The lag time from the starting of rainfall to onset of runoff generation was <20 min and the topsoil was still unsaturated. Mechanism of the infiltration excess runoff therefore can be inferred that is the rain intensity $\geq 2.6 \text{ mm} \times 5 \text{ min}^{-1}$.

Figures 5 and 6 also show that ephemeral runoff is unstable and the magnitude was significantly influenced by intensity of rain. Runoff normally maintained transitory existence and disappeared soon after the rain ceased.

Correlation between rainfall factors and runoff rate

Some rainfall-runoff events were randomly selected to estimate the relationships between rainfall factors and runoff rate, and the results are listed in Table 1 (ESM only). The regression curve of average intensity of rain and

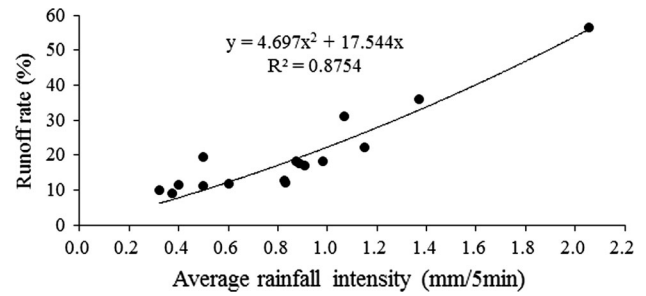


Fig. 7 Relationship between average rain intensity and runoff rate

Table 2 Index of annual precipitation and runoff rate

Year	Precipitation (mm)	Runoff (m ³)	Runoff rate (%)
2005	315.0	710	2.5
2006	386.0	6,600	18.0
2007	481.0	6,500	15.0
2008	502.0	3,500	7.8
2009	511.0	5,000	10.8
Average	439	4,462	11.0

The calculated area is the catchment of the surface flow observed area (about 0.1 km²)

runoff rate of the events in Table 2 are shown in Fig. 7. The curve indicates that high correlation (>0.87) exists between average intensity of rain and runoff rate. Both relationships between rainfall duration and runoff rate and amount of rainfall and runoff rate were also evaluated, there is no conspicuous relationship between rainfall duration and runoff rate (Fig. 2, ESM only), as well as between amount of rainfall and runoff rate (Fig. 3, ESM only). Therefore, among rainfall factors of average rain intensity, rainfall duration and amount of rainfall, average intensity is a key factor which impacts runoff rate of every runoff event.

Annual runoff rate

Calculation of rainfall-runoff was carried out using numerical method (Eqs. 1–4), model lumping: Fig. 2) for 5 years (2005–2009). Data processed covered the period in which there was runoff generation. The results of annual precipitation, runoff and runoff rate are summarized in Table 2.

In 2005, because the precipitation was less than the annual mean and few intensive rainfall events occurred which resulted in three surface runoff events with low runoff rates. In 2006, though the amount of precipitation was evidently lower than the annual mean, due to concentrated rainfall mainly in the rainy season and the high occurrence of intensive rainfall events, there has been relatively high runoff. In 2007, precipitation was slightly

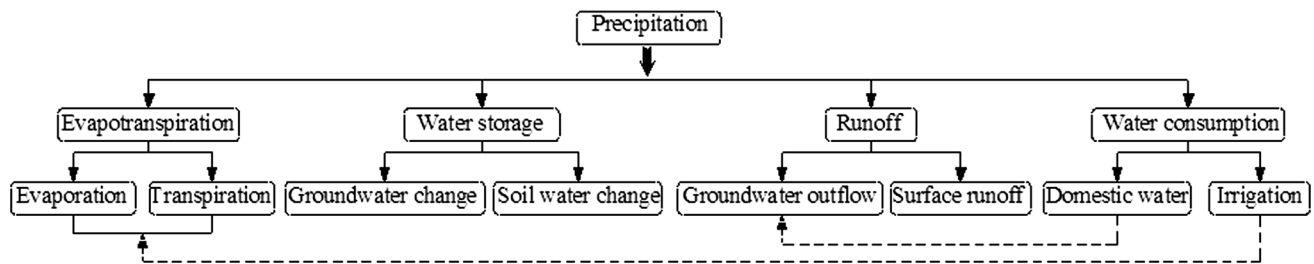


Fig. 8 Diagram of annual water budget at the study location

more than the annual mean and its annual distribution approximately represented the normal year as most part was received in the rainy season in the form of several intensive rainfall events with relatively high intensity, therefore, runoff rate in 2007 was approximately equated to the annual mean value. In 2008, though precipitation was visibly higher than annual mean and was approximate to that of 2007, owing to lack of heavy rainfall event, runoff rate was less than that of 2007. In 2009, precipitation was approximate to that of 2008 but runoff rate was higher than that of 2008 due to differences in seasonal rainfall distribution between 2008 and 2009.

Mean annual precipitation in given years (2005–2009) was 439 mm which was approximately equal to the annual mean (430 mm a⁻¹), while the average runoff rate was 11.0 %. Based on results of average annual runoff rates for 5 years (2005–2009), annual runoff rate at the study location can be estimated as 10–15 %.

Annual water budget

Water budget equation

Water budget relationship at the earth's surface is complex and dynamic. The relationship involves interactions between atmosphere, surface, soil, plant and groundwater. Main components of the hydrologic circle are precipitation, runoff, infiltration, and evapotranspiration (Eagleson 1970; Huang et al. 2001). Analysis of the water balance is the basis for realizing the scientific evaluation and appropriate allocation of the water resources in a basin (Zhu et al. 2008). The results of the field observation and numerical results of the surface runoff for 5 years (2005–2009) were used for estimating the annual water budget of the Liudaogou Catchment. To emphasize target value of each water budget component, the unit area of 1 km² was selected as the index area. Considering habitant water consumption at the study location, a new factor U was added to the common water budget formula (Eq. 5).

$$P = R + \Delta W + E + U \quad (5)$$

where, P is the precipitation, R is the runoff which includes surface runoff and groundwater outflow, ΔW is the change

of water storage in a basin which manifests in variation of soil water content and the change of groundwater, its annual mean value is approximate to 0, E is evapotranspiration, U is the habitant water consumption, it includes domestic water and irrigation water at the Liudaogou Catchment.

The general distribution of water to components of water budget in the study location is depicted by a schematic illustration shown in Fig. 8. In the natural state, the water resources in a catchment maintain a normal sustainable state and keep a dynamic balance. However, if the water balance in a basin is distributed by water resources development and by human activities, such as groundwater overdraft for farmland irrigation, the change of water storage, ΔW , will lead to negative value or deficit state (Todd and Mays 2005; Yu 2008).

Each component of annual water budget

Precipitation

For a closed basin, the total water inflow refers to the precipitation received during the period of analyzes. Thus, average annual precipitation of 430 mm is the total water inflow to the study location in a normal year.

Runoff

Annual runoff includes surface runoff and groundwater outflow.

Average annual surface runoff rate for 5 years (2005–2009) was estimated at 11.0 % based on the numerical results of runoff calculation. As mean annual precipitation for the 5 years (2005–2009) was 439 mm, which is almost equal to the annual mean, surface runoff rate of 11.0 % was adopted as the annual runoff rate in the normal year and it is equivalent to rainfall of 47.3 mm a⁻¹.

Observation of groundwater outflow was carried out and the observational point was as shown in Fig. 1c. Groundwater flow occurs at the phreatic zone and its discharge gradually increases from the observational position to the downstream. Discharge of groundwater flow was observed using a flow meter and the observed results indicated that

the groundwater outflow was relatively stable at the observational point and did not show distinct change in spite of seasonal changes. The mean discharge throughout the observed time was about $1.77 \times 10^3 \text{ cm}^3 \text{ s}^{-1}$. However, groundwater outflow seasonally ceased in winter from December to the end of February due to the upper ground was frozen.

The Liudaogou Catchment can be treated as hydrogeological homogeneous model due to its uniform ground condition (Zheng et al. 2005). The groundwater flow is therefore considered to be uniformly generated from each tributary. On account of the catchment area of the discharge observed point is 1.04 km^2 , discharge of groundwater outflow from the unit area is estimated to be $1.70 \times 10^3 \text{ cm}^3 \text{ s}^{-1}$ and its annual amount is $4.04 \times 10^4 \text{ m}^3 \text{ a}^{-1}$ (converted to millimeter, 40.4 mm a^{-1}).

Change of water storage

According to actual investigation at the study location, deep groundwater generally lies at depth of dozens of meters or even over a hundred meters from the ground surface. On the other hand, annual rainfall is mainly concentrated to the rainy season during which intense evapotranspiration consumes most of the soil water. Therefore, deep groundwater cannot get effective recharge from rainwater infiltration (Fan 2005). Annual water storage was thought to vary mainly with variation of the soil water content and change of the shallow groundwater (phreatic water).

The soil water content data were provided by the previous research activities at the same study location (Kimura et al. 2005b). The observed point was shown in Fig. 1c. In the study location, evapotranspiration impacts the infiltration to the maximum depth of 60 cm from the ground surface and the soil water content remains relatively stable below this depth (Fan 2005). The observational depth of the soil water content was 4, 10, 26, 34, 42, 50, 58 66 cm and at the maximum depth of 100 cm. The results of the average soil water content at various depths indicate that mean soil water content maintained the same level at the beginning and end of each year such as on 1st January 2005, 2006 and 2007, soil water content is 0.0761, 0.076 and $0.0764 \text{ cm}^3 \text{ cm}^{-3}$, respectively (Fig. 4, ESM only). Therefore, annual water storage response to variation of soil water content can be estimated to be 0.

Observation of shallow groundwater was carried out at a site (well No. 1) as shown in Fig. 1c. The observed results of groundwater fluctuation and mean monthly groundwater change during the observed time represents that groundwater maintains the same level at the annual corresponding time such as on 16 March 2005 and 2006, groundwater level was 1.465 and 1.467 m, respectively, and

groundwater change is approximately 0 at the beginning and end of each year (Fig. 5a, b, ESM only). Thus, annual groundwater change remains constant.

Based on the analysis results of annual variation of soil water content and groundwater change, annual change of water storage is approximately 0 at the study location.

Water consumption

Water consumption in the Liudaogou Catchment includes domestic water and irrigation water.

Irrigation water was provided by two reservoirs, large and small as shown in Fig. 1c. The large reservoir supplied 70 % of the annual irrigation water requirement and the small one supplied 30 % of the balance requirement. The irrigation period was from late April to September almost covering the whole growing season. Amount of irrigation water withdrawal is roughly estimated by the change of the water level in the reservoirs. Method for estimating irrigation water withdrawal is to evaluate fall of water level from the original water level in the large reservoir as shown in Fig. 6a (ESM only). Monthly distribution of the irrigation water withdrawal from the large reservoir is shown in Fig. 6b (ESM only) which represents the irrigative process and the amount of irrigation water remained same in all 3 years (2006–2008). Based on the estimated irrigation water withdrawal from the large reservoir, amount of irrigation water provided by the small reservoir in the corresponding year was estimated to be $1.0 \times 10^4 \text{ m}^3$ (in 2006 and 2007) and $1.06 \times 10^4 \text{ m}^3$ (in 2008). The total irrigated area is 20.6 hm^2 which is equivalent to $3.0 \text{ hm}^2 \text{ km}^{-2}$ in the Liudaogou Catchment and annual amount of irrigation water is 5.1 mm of annual precipitation.

Domestic water normally includes water supply for residents and cattle. The domestic water is supplied by an artesian well at the upstream of the Liudaogou Catchment (well No. 2 in Fig. 1c). Groundwater in this well also belongs to the phreatic water. Based on the observed result of water level in well No. 2 (the data is discontinuous) and actual investigation on local water utilization, amount of daily domestic water requirement was 200 m^3 and this increased to 300 m^3 in summer from July to September. Total annual domestic water was estimated to 12 mm of annual precipitation.

Evapotranspiration

Evapotranspiration generally refers to the sum of evaporation from ground surface and transpiration from vegetation. In view of the complicated geomorphological features of the study location such as the bare land, the crops, and various types of vegetation, actual

Table 3 Components of annual water budget (unit area: 1 km²)

Components	Precipitation (<i>P</i>)	Evapotranspiration (<i>E</i>)	Runoff (<i>R</i>)		Water utilization (<i>U</i>)		Water storage ΔW
			Surface	Groundwater	Domestic	Irrigation	
Amount (mm)	430	324.2	47.3	40.4	12.0	5.1	0
Percentage (%)	100	75.6	20.4		4.0		0

evapotranspiration is difficult to estimate accurately. Based on hydrological principle for water budget in a closed basin, its annual change of water storage is 0 and the water output consists of evaporation and runoff (Zhu et al. 2008; Li et al. 2011). Based on the estimated results of annual variation of the soil water content and groundwater change, which are both equal to 0 at the study location, annual evapotranspiration was approximately estimated by subtracting surface runoff, groundwater outflow, and water consumption from annual precipitation. And it is 324.2 mm over the unit area.

Index of annual water budget

Index (%) of annual water budget is listed in Table 3. Total annual runoff (surface and groundwater), annual water consumption, and annual change of water storage account for 20.4, 4.0 and 0 % of the total annual precipitation, respectively, while annual evapotranspiration represents 75.6 % of the annual precipitation. From view point of the total hydrological cycle, annual irrigation water use can generally be regarded as a part of evapotranspiration (Fig. 8) which resulted in evapotranspiration attaining 76.8 % of the annual precipitation. Domestic water can be considered as a part of groundwater outflow (Fig. 8) with the result that annual runoff accounted for 23.2 % of the annual precipitation.

Precipitation is supposed to be utilized efficiently by means of the proper methods, however, it is viewed as impossible under the current conditions. In view of the existing conditions at the wind–water erosion crisscross region on the northern Loess Plateau such as complex landform, intense evapotranspiration in summer and the underdeveloped economy, efficient utilization of precipitation and the surface runoff is difficult. Therefore, the shallow groundwater combined with its outflow becomes the significant available water resources for agricultural production and people's daily lives.

Conclusions

In this study, the observed hydrological data and numerical results of the surface flow were used for evaluating the main runoff characteristics and annual water budget for the

Liudaogou Catchment on the northern Loess Plateau. Some conclusions were drawn as follows:

For the characteristics of ephemeral runoff:

- (1) Mechanisms of runoff generation were clarified by analyzing the representative rainfall combined with runoff and change of soil water content in the same period. The conditions of runoff generation for saturated topsoil and unsaturated topsoil are intensity of rain $\geq 0.6 \text{ mm} \times 5 \text{ min}^{-1}$ and $\geq 2.6 \text{ mm} \times 5 \text{ min}^{-1}$, respectively.
- (2) A relatively high correlation existed between the runoff ratio and average rainfall intensity, runoff ratio was proportional to the average rainfall intensity.
- (3) Based on the annual runoff rate of 2005–2009 which achieved by numerical analysis of the rainfall-runoff, annual runoff rate of the Liudaogou Catchment was estimated to be 10–15 %.

For annual water budget:

Annual runoff, evapotranspiration, change of water storage, and water consumption accounted for 20.4, 75.6, 0 and 4 % of annual precipitation, respectively. Evapotranspiration is much more predominant than other hydrological factors in annual hydrological circle at the wind–water erosion crisscross region on the northern Loess Plateau.

Acknowledgments The authors gratefully acknowledge the financial support from National Natural Science Foundation of China (NSFC) (No. 41271046), JSPS (Japan Society for the Promotion of Science) Core University Program, Postdoctoral Science Foundation of China for overseas scholar (No. 87328), and Heilongjiang Provincial Department of Education Scientific Research Foundation for overseas scholars, China (No. 1251H017).

References

- Abbott MB, Bathurst JC, Cunge JA et al (1986) An introduction to the European hydrological system—systeme hydrologique Europeen, SHE2. Structure of physically-based distributed modeling system. *J Hydrol* 87:61–77
- Bo W, Long J (2002) Land change and desertification development in the Mu-Uss sand land, north China. *J Arid Environ* 50:429–444
- Bu YS, Shao HL, Wang JC (2002) Effects of different mulching materials on corn seedling growth and soil nutrients' contents and

- distributions. *J Soil Water Conserv* 16(3):40–42 (in Chinese with English abstract)
- Calver A, Wood WL (1995) The Institute of hydrology distributed model. In: Singh VP Chapter 17 in computer models of watershed hydrology. Water Resources Publications, Littleton
- Chen LD, Huang ZL, Gong J et al (2007) The effect of land cover/vegetation on soil water dynamic in the hilly area of the Loess Plateau, China. *Catena* 70(15):200–208
- Chua Lloyd HC, Wong Tommy SW, Sriramula LK (2008) Comparison between kinematic wave and artificial neural network models in event-based runoff simulation for an overland plane. *J Hydrol* 357:337–348
- Ciarapica L, Todini E (2002) TOPKAPI: a model for the representation of the rainfall-runoff process at different scales. *Hydrol Process* 16:207–229
- Delfs JO, Wang W, Kalbacher T et al (2013) A coupled surface/subsurface flow model accounting for air entrapment and air pressure counterflow. *Environ Earth Sci* 69(2):395–414
- Eagleson P (1970) *Dynamic hydrology*. McGraw Hill, New York
- Fan J (2005) Study on the soil water dynamics and modeling in water-wind erosion crisscross region on the Loess Plateau. Dissertation. Institute of Soil Science, CAS, China (in Chinese)
- Fan J, Shao MA, Wang QJ (2006) Soil water restoration of alfalfa land in the wind–water erosion crisscross region on the Loess Plateau. *Acta Agraria Sinica* 13(3):261–264 (in Chinese with English abstract)
- Fan J, Shao MA, Wang QJ (2010) Toward sustainable soil and water resources use in China’s highly erodible semi-arid Loess Plateau. *Geoderma* 155:93–100
- Hu W, Shao MA, Han FP et al (2011) Spatio-temporal variability behavior of land surface soil water content in shrub- and grassland. *Geoderma* 162:260–272
- Huang MB, Shao MA, Li YS (2001) Comparison of a modified statistical-dynamic water balance model with the numerical model WAVES and field measurements. *Agric Water Manag* 48:21–35
- Huang JB, Hinokidani O, Yasuda H et al (2008) Study on characteristics of the surface flow of the upstream region in Loess Plateau. *Ann J Hydraul Eng JSCE* 52:1–6
- Huang JB, Wang B, Hinokidani O et al (2011) Application of kinematic wave model to calculate “rainfall-runoff” process at hilly-gully region in the Loess Plateau, China. Proceeding of 2011 international symposium on water resource and environmental protection 5:422–425
- Huang JB, Hinokidani O, Yasuda H et al (2013) Effects of the check dam system on water redistribution in the Chinese Loess Plateau. *J Hydrol Eng* 18(8):929–940
- Huo Z, Shao MA, Horton R (2008) Impact of gully on soil moisture of shrub land in wind–water erosion crisscross region of the Loess Plateau. *Pedosphere* 18(5):674–680
- Japan Society of Mechanical Engineers (1988) *Fundamentals of computational fluid dynamics*. Corona, Tokyo (in Japanese)
- Jia XX, Shao MA, Wei XR et al (2010) State-space simulation of soil surface water content in grassland of northern Loess Plateau. *Trans CSAE* 26(10):38–44 (in Chinese with English abstract)
- Jiang N, Shao MA, Lei TW et al (2005) Spatial variability of soil infiltration properties on natural slope in Liudaogou Catchment on Loess Plateau. *J Soil Water Conserv* 19(1):14–17 (in Chinese with English abstract)
- Kimura R (2007) Estimation of moisture availability over the Liudaogou river basin of the Loess Plateau using new indices with surface temperature. *J Arid Environ* 70:237–252
- Kimura R, Okada S, Miura H et al (2004) Relationships among the leaf area index, moisture availability, and spectral reflectance in an upland rice field. *Agric Water Manag* 69:83–100
- Kimura R, Liu Y, Takayama N et al (2005a) Heat and water balances of the bare soil surface and the potential distribution of vegetation in the Loess Plateau, China. *J Arid Environ* 63:439–457
- Kimura R, Fan J, Zhang XC et al (2005b) Evapotranspiration over the grassland field in the Liudaogou basin of the Loess Plateau, China. *Acta Oecologica* 29:45–53
- Kimura R, Bai L, Fan J et al (2007) Evapotranspiration estimation over the river basin of the Loess Plateau of China based on remote sensing. *J Arid Environ* 68:53–65
- Li YS (1983) The properties of water cycle in soil and their effect on water cycle for land in the loess region. *Acta Ecologica Sinica* 3(2):91–101 (in Chinese)
- Li WY, Zhang W, Ge JM et al (2011) Water balance analysis method and its application. *Water Resour Prot* 27(6):83–87 (in Chinese)
- Lu CH, van Ittersum MK (2004) A trade-off analysis of policy objectives for Ansai, the Loess Plateau of China. *Agric Ecosys Environ* 102:235–246
- Mariza CC, Luis G, Rafael LB et al (1992) A kinematic model of infiltration and runoff generation in layered and sloped soils. *Adv Water Resour* 15:311–324
- Neitsch SL, Arnold JG, Kiniry JR et al (2000) Soil and water assessment tool theoretical documentation (version 2000). <http://www.brc.tamus.edu/SWAT/>
- Sarkar R, Dutta S (2012) Field investigation and modeling of rapid subsurface storm flow through preferential pathways in a vegetated hillslope of northeast India. *J Hydrol Eng* 17(2):333–341
- Shi H, Shao MA (2000) Soil and water loss from the Loess Plateau in China. *J Arid Environ* 45:9–29
- Tang KL (2000) Importance and urgency of harnessing the interlocked area with both water and wind erosion in the Loess Plateau. *Soil Water Conserv China* 11:11–17 (in Chinese)
- Todd DK, Mays LW (2005) *Groundwater Hydrology*. John Wiley & Sons, Inc, Hoboken
- Wang Q, Takahashi H (1999) A land surface water deficit model for an arid and semiarid region: impact of desertification on the water deficit status in the Loess Plateau, China. *J Clim* 12:244–257
- Wang YQ, Fan J, Shao MA (2010) Rules of soil evaporation and millet evapotranspiration in rain-fed region of Loess Plateau in northern Shaanxi. *Trans CSAE* 26(1):6–10 (in Chinese with English abstract)
- Yang WX (1996) The preliminary discussion on soil desiccation of artificial vegetation in northern regions of China. *Scientia Silvae Sinicae (China)* 32:78–84 (in Chinese with English abstract)
- Yang WZ, Shao MA (1998) On the relationship between environmental aridization of the Loess Plateau and soil water in loess. *Sci China (Series D)* 28(4):357–365
- Yomoto A, Mohammad NI (1992) Kinematic analysis of flood runoff for a small-scale upland field. *J Hydrol* 137:311–326
- Yu WD (2008) Water balance and water resources sustainable development in Haihe river basin. *J China Hydrol* 28(3):79–82 (in Chinese with English abstract)
- Zheng JY, Shao MA, Li SQ (2005) Variation of the hydraulic characteristics of the soil profile in water-wind erosion crisscross region. *Trans CSAE* 21(11):64–66 (in Chinese with English abstract)
- Zhu YJ, Shao MA (2008) Variability and Pattern of surface moisture on a small-scale hillslope in Liudaogou Catchment on the northern Loess Plateau of China. *Geoderma* 147:185–191
- Zhu XJ, Wang ZG, Xia J (2008) Basin level water balance analysis study based on distributed hydrological model—case study in the Haihe river basin. *Prog Geogr* 27(4):23–27 (in Chinese with English abstract)